

# PULSED HIGH-ENERGY RADIATION FROM OBLIQUE MAGNETIC ROTATORS

A. FERRARI and E. TRUSSONI

*Laboratorio di Cosmo-geofisica del CNR and Istituto di Fisica  
Generale dell'Università, Torino, Italy*

(Received 8 July, 1974)

**Abstract.** A detailed analysis is reported of charged particle motion in the e.m. fields generated by oblique magnetic rotators. A full treatment of particle trajectories, radiated power and spectrum is given; astrophysical implications of these results in connection with pulsars, mainly NP 0532, are discussed and the possibility of a high energy pulsed radiation model with synchro-Compton emission at the speed-of-light cylinder is investigated.

## 1. Introduction

The high efficiency of the process of charged particle acceleration by large amplitude electromagnetic waves emitted by pulsars in the scheme of the oblique magnetic rotator theory was emphasized by Ostriker and Gunn in their original paper of 1969.

Since then many authors have discussed various physical aspects of this interaction in connection with galactic and extragalactic problems; in particular the radiation emission from particles accelerated by strong waves, the so-called synchro-Compton process (Gunn and Ostriker, 1971; Ferrari and Trussoni, 1971), was tentatively applied to models for the pulsars themselves (Grewing and Heintzmann, 1971), the Crab nebula (Rees, 1971b) and extragalactic extended radio-sources (Rees, 1971a; Blandford and Rees, 1972). However, these preliminary evaluations are seriously biased by several inadequacies. Therefore in the present note we want to give a detailed discussion of trajectories, emitted power and radiation spectrum of charged particles moving in strong fields generated by magnetic rotators with special interest to the validity of a pulsar model based on the synchro-Compton emission by electrons (and protons) accelerated from the region where corotation (with rotator) breaks off, i.e., the speed-of-light distance,  $R_c = c/\omega$ .

Standard assumptions for electrodynamic pulsar models are listed here for future reference.

(1) Pulsars are rotating collapsed stars with strong magnetic fields at their surface; typical values of parameters for young pulsars, like NP 0532, are:  $M \approx 1 M_\odot$ ,  $R \approx 10$  km,  $\omega \approx 200$  rad s<sup>-1</sup>,  $B_s$  (surface magnetic induction)  $\approx 10^{10-12}$  G. The structure of the magnetic field is axially symmetric (e.g. dipolar).

(2) Simple electrodynamic estimates require the existence of magnetospheres around magnetic rotators; this plasma is corotating within a distance  $r \lesssim c/\omega$  (for dense magnetospheres  $r \lesssim V_A/\omega$ ,  $V_A$  being their Alfvén velocity), but open magnetic

lines exist allowing a particle leakage, or ‘wind’. Then at  $r \approx c/\omega$  these particles are caught by the strong fields of the rotator, which have become travelling waves. This interaction is typically a single particle process for the appropriate parameters; in fact strong waves are not absorbed (nor refracted), since electromagnetic pressure largely exceeds plasma kinetic pressure. On the other hand the field structure is rather complex and the simplification used so far actually leads to underestimating radiative effects.

In the next three sections we shall work out a suitable physical model to enlighten the peculiar effects arising from a rather general configuration of rotator’s fields. Then a final discussion will be presented of results relevant to astrophysical models of young, energetic pulsars.

## 2. Equations of Motion and Electromagnetic Field Structure

The relativistic equations of motion of charged particles acted upon by electromagnetic fields are the classical Lorentz-Dirac equations

$$ma^\mu = \frac{e}{c} F^{\mu\nu} v_\nu + \Gamma^\mu, \quad (1)$$

where  $m$  is the rest mass,  $F^{\mu\nu}$  the electromagnetic tensor,  $a^\mu$  the four-acceleration,  $v_\nu$  the four-velocity and

$$\Gamma^\mu = \frac{2}{3} \frac{e^2}{c^3} \left( \dot{a}^\mu - \frac{1}{c^2} a^\lambda a_\lambda v^\mu \right) \quad (2)$$

is the relativistic radiation reaction force (all time derivatives are with respect to proper time). For relatively small amplitude electromagnetic fields,  $\Gamma^\mu$  is a negligible correction in Equation (1) and the classical treatment is always correct. Conversely for the standard values of pulsar parameters  $\Gamma^\mu$  can become important since fields are large enough to accelerate particles to relativistic velocities in the characteristic time of oscillations; i.e. their strength parameter (Lorentz invariant) is

$$f = \frac{eB_0}{mco} \gtrsim 1 \quad (B_0 \text{ field amplitude}). \quad (3)$$

In this case the interaction is highly non-linear and fully relativistic, and Equation (1) is valid only for  $f$  not exceedingly large: namely,

$$f \lesssim \gamma^{-1} (\lambda_{\text{inc}}/\lambda_C), \quad (4)$$

where  $\gamma$  is the particle Lorentz factor,  $\lambda_C$  their Compton wavelength and  $\lambda_{\text{inc}}$  the wavelength of the incident field. It will be shown later that  $\gamma \approx 0.1f$ , so that standard pulsar parameters quoted above allow a classical treatment of the problem and all physical aspects of the non-linear interaction are considered adequately, without necessarily referring to the less intuitive formalism of quantum electrodynamics. In this framework

perturbative methods lead us to write Equations (1)–(2) in terms of the incident fields only. In an inertial frame centred on the rotating dipole the equations of motion were put in the following scalar form, using spherical coordinates,

$$\left. \begin{aligned}
 \frac{dp_r}{dt} &= \frac{m\gamma}{r} (v_\theta^2 + v_\phi^2) + \frac{e}{c} (B_\phi v_\theta - B_\theta v_\phi + cE_r) - \\
 &\quad - \tau_0 r_e \frac{v_r}{c} \gamma^2 F^2, \\
 \frac{dp_\theta}{dt} &= -\frac{m\gamma}{r} (v_r v_\theta - v_\phi^2 \operatorname{ctg} \vartheta) + \frac{e}{c} (B_r v_\phi - B_\phi v_r + cE_\theta) - \\
 &\quad - \tau_0 r_e \frac{v_\theta}{c} \gamma^2 F^2, \\
 \frac{dp_\phi}{dt} &= -\frac{m\gamma}{r} (v_r v_\phi + v_\theta v_\phi \operatorname{ctg} \vartheta) + \frac{e}{c} (B_\theta v_r - B_r v_\theta + cE_\phi) - \\
 &\quad - \tau_0 r_e \frac{v_\phi}{c} \gamma^2 F^2,
 \end{aligned} \right\} \quad (5)$$

where

$$\begin{aligned}
 p_i &= m\gamma v_i = \text{relativistic momentum components,} \\
 F^2 &= (\mathbf{E} + (\mathbf{v}/c) \times \mathbf{B})^2 - (1/c^2)(\mathbf{E} \cdot \mathbf{v})^2, \\
 r_e &= e^2/mc^2 = \text{classical radius of electrons,} \\
 \tau_0 &= \frac{2}{3}(r_e/c) = \text{limiting time scale for classical electrodynamics.}
 \end{aligned}$$

Numerical codes do actually include other terms for radiation braking which are generally negligible in relativistic regimes ( $\gamma \gtrsim 1$ ). In addition the impossibility must be noticed of scaling down the problem because of the importance of radiation reaction itself.

Referring now to the analytical expressions for the electromagnetic field components, we recall that three distinct regions exist around any magnetic rotator: (i) an inner zone, between the stellar surface,  $r=a$ , and the speed-of-light radius,  $r \approx c/\omega$ , where magnetic forces prevail over electric forces ( $B \gg E$ ), and particles, extracted from the star by large longitudinal (to  $B$ ) electric field  $E_{\parallel}$ , are forced to corotate almost rigidly; (ii) an intermediate zone,  $r \approx c/\omega$ , where  $E$  can be larger than  $B$  (near fields), favouring electrostatic acceleration processes and cancelling corotation; (iii) an outer zone,  $r \gg c/\omega$ , where electromagnetic fields become outwards travelling spherical waves and support an efficient electromagnetic acceleration.

These general features hold for any magnetic structure assumed at the star's surface and do not depend upon the charge distribution which is consistently created in region (i). Therefore we are reasonably allowed to adopt a simple configuration, i.e. magnetic dipole, which does already contain all physical ingredients significant for a pulsar model, namely regions where  $E > B$  outside the corotating magnetosphere. In addition

we must recall that a field structure around a dipole rotator (for general orientation of magnetic and spin axes) which takes into account self-consistently the charge distribution in region (i), has not been given so far; the only analytical solution available for our computations is the one by Deutsch (1955) for a magnetic dipole rotating in vacuo (or in a tenuous magnetosphere as shown by Ferrari and Trussoni, 1973), but we shall discuss how the main results are applicable to general configurations.

The electromagnetic fields of a rotating magnetic dipole in vacuo with magnetic and spin axes at angle  $\chi$  were written in the inertial frame centered on the star:

$$\left. \begin{aligned} B_r &= B_a \left[ \left( \frac{a}{r} \right)^2 B_1(r, \eta) \sin \vartheta \sin \chi + \left( \frac{a}{r} \right)^3 \cos \chi \cos \vartheta \right], \\ B_\vartheta &= \frac{B_a}{2} \left[ \frac{a}{r} B_2(r, \eta) \cos \vartheta \sin \chi + \left( \frac{a}{r} \right)^3 \cos \chi \sin \vartheta \right], \\ B_\varphi &= \frac{B_a a}{2 r} B_3(r, \vartheta, \eta), \\ E_r &= \frac{B_a}{2} \left[ 3 \left( \frac{a}{r} \right)^2 E_1(r, \eta) \sin 2\vartheta \sin \chi - \frac{1}{2} \left( \frac{a}{r} \right)^4 \cos \chi (3 \cos 2\vartheta + 1) \right], \\ E_\vartheta &= \frac{B_a}{2} \left[ \frac{a}{r} E_2(r, \vartheta, \eta) \sin \chi - \left( \frac{a}{r} \right)^4 \sin 2\vartheta \cos \chi \right], \\ E_\varphi &= \frac{B_a}{2} E_3(r, \eta) \cos \vartheta \sin \chi, \end{aligned} \right\} \quad (6)$$

where

$$\eta = \varphi - \omega \left( t - \frac{r-a}{c} \right),$$

and  $B_1, B_2, B_3, E_1, E_2, E_3$  are known positional functions (see Ferrari and Trussoni, 1973).

In addition the extension of the corotating magnetosphere must be defined, i.e. the speed-of-light cylinder. The radius of this cylinder is obviously  $\approx R_c = c/\omega$  and its height has to be of the same size referring to magnetic field lines which do 'close' inside the corotating magnetosphere (see Figure 1).

The cylinder defines the region where the electromagnetic acceleration begins in the assumption that the corotating magnetosphere can be considered in a quasi-equilibrium state between particle evaporation from the star and particle loss at the external boundary.

It is clearly implicit in our treatment that absorption and refraction of waves outside the corotating region by streaming particles be completely negligible, so that also collective effects are unimportant (single particle interaction).

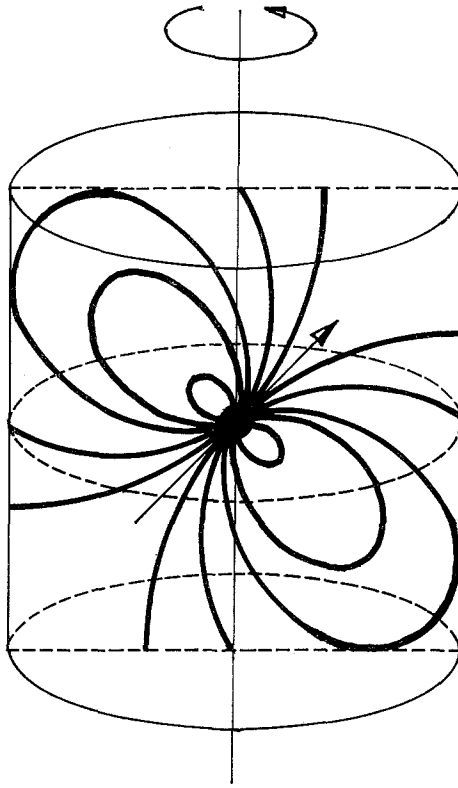


Fig. 1. Schematic representation (not to scale) of speed-of-light cylinder for an oblique magnetic dipole.

### 3. Particle Motion in the Fields of Magnetic Rotators

Before discussing the main features of particle trajectories, we recall that, for any electromagnetic field structure, three main components are at work in their dynamics: (i) gyration around magnetic flux lines; (ii) electric drift along the Poynting vector; (iii) electrostatic sliding along magnetic flux lines (additional drifts are not relevant to this discussion). It is well known that for  $E/B \ll 1$  a particle trajectory is correctly described in the guiding centre approximation and velocities are not relativistic. Conversely in our problem  $E/B$  is of the order of unity (and  $|E - B|/|E + B| \ll 1$ ); the motion is still determined by the three components above, but becomes relativistic, and in particular an important role is played by  $E_{\parallel}$ , electric field component parallel to  $B$ .

It is useful to discuss separately the motion in the fields of perpendicular ( $\chi = \pi/2$ ) and oblique ( $\chi = \pi/4$ ) rotators.

#### 3.1. PERPENDICULAR MAGNETIC ROTATORS

Equations (6) show that the ratio  $E/B$  has different values in the region  $r \approx R_c$ : it

increases with the latitude from the equator (where  $E/B \lesssim 0.45$ ) to the poles (where  $E/B \sim 1.4$ ); at intermediate latitudes the configuration in longitude shows a pattern of zones with  $E/B > 1$  and  $< 1$  alternatively, whose amplitude is  $\vartheta$ -dependent. In particular,  $E_{\parallel}$  varies with latitude, being null at the equator and increasing with latitude (positive and negative). Other obvious symmetries exist, but – although suggestive – they do not uniquely determine the particle trajectories.

Actually field symmetries can drive the initial stages of the acceleration only and not the asymptotic part of trajectories, and in addition fields become antisymmetric when  $\varphi$  is rotated by  $\pi$  radians; thus the drift velocity does not change direction, while the  $E_{\parallel}$  pull reverses its sign: therefore trajectories with starting points differing by  $\pi$  in longitude do not share any similarity, yet having an equal ratio  $E/B$ .

Two significant ranges of initial colatitudes can be singled out:  $0 \leq \vartheta_0 \leq \pi/4$  and  $\pi/4 < \vartheta_0 \leq \pi/2$  (injections at  $\pi/2 < \vartheta_0 \leq \pi$  give symmetrical results). Then, recalling our

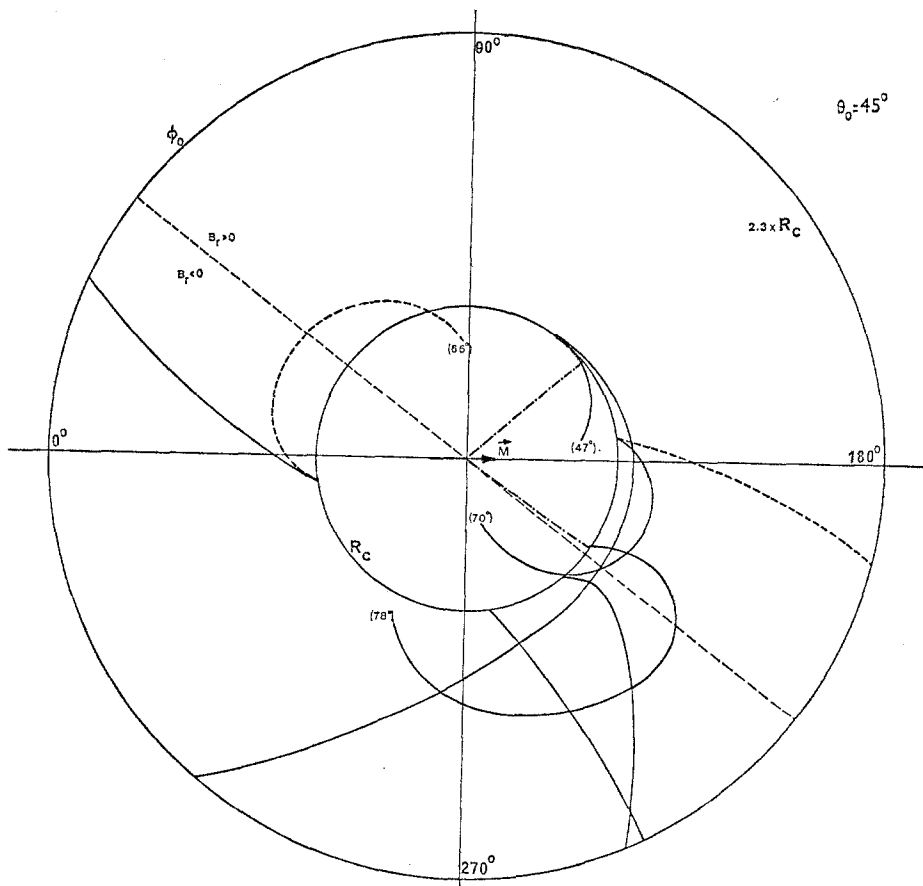


Fig. 2. Projection of particle trajectories onto the equatorial plane for injection at  $\vartheta_0 = \pi/4$ . Full lines: electrons; dotted lines: protons. Sketched – dotted lines limit the FS (forbidden sector); numerical figures in brackets are asymptotic colatitudes  $\vartheta$  for particles injected in the FS.

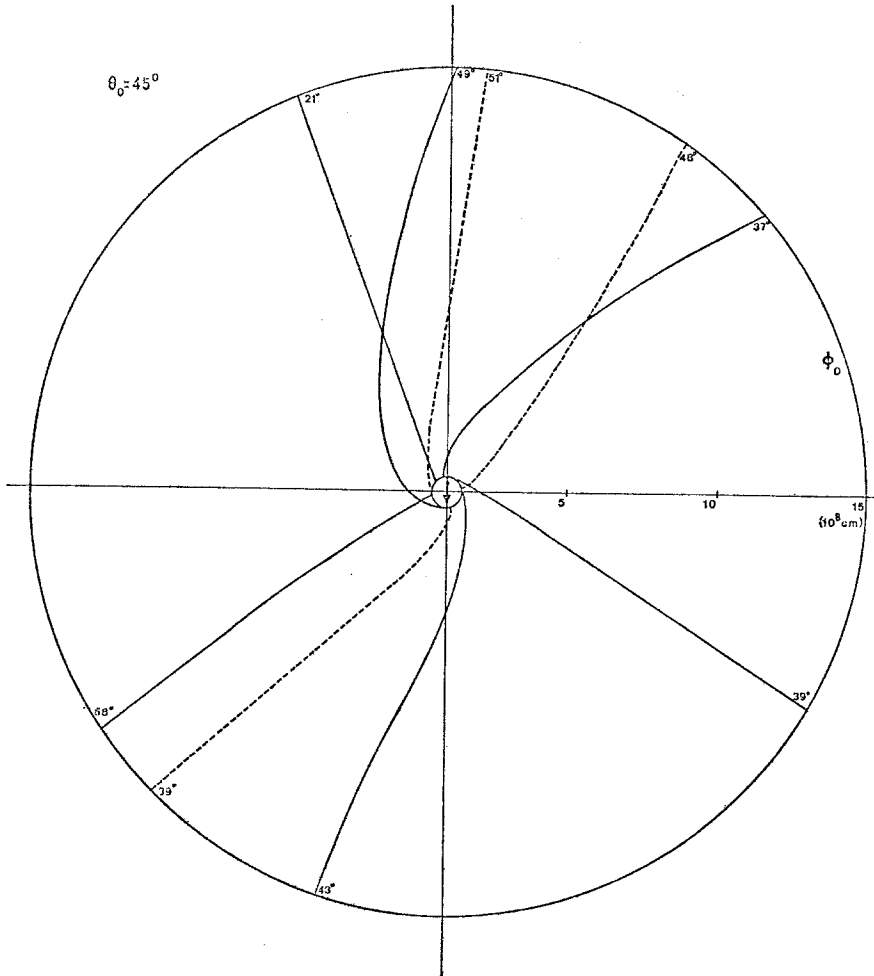


Fig. 3. Asymptotic part of trajectories for the same case of Figure 2. Labelling of trajectories gives asymptotic values for  $\vartheta$ .

definition of light cylinder based on the condition that open field lines exist carrying particles outside corotating regions (see Figure 1), the initial values of radial coordinates must be assumed:

$$r_0 = R_c / \sin \vartheta_0 \quad \text{for } \vartheta_0 \geq \pi/4 \quad (\text{equatorial}),$$

$$r_0 = R_c / \cos \vartheta_0 \quad \text{for } \vartheta_0 \leq \pi/4 \quad (\text{polar}).$$

In Figures 2 and 3 trajectories of electrons (full lines) and protons (dotted lines) injected at rest at  $\vartheta_0 = \pi/4$  are shown as projected (in the inertial frame) on a plane parallel to the equator.

We note the following main features, mainly referring to electrons:

- (1) For azimuthal injection angles  $0^\circ \leq \varphi_0 \leq 140^\circ$  (with respect to magnetic axis)

electrons acquire initially a large azimuthal velocity and move almost tangentially to the light cylinder ( $\vartheta \approx \text{const}$  asymptotically), since electric drift and sliding have opposite sign in the radial direction.

(2) For  $140^\circ \leq \varphi_0 \leq 220^\circ$ , including the south magnetic pole direction,  $E_{\parallel} > 0$  and drift velocities point toward the star; thus electrons (if injected at  $R_c$ ) are pushed back into the corotating region, where motion is eventually driven along magnetic lines being  $E \ll B$ . This means that a magnetospheric 'forbidden sector' (FS) for electron ejection is present. A symmetrical region exists for protons (or positive ions), captured about the north magnetic pole.

(3) For  $220^\circ \leq \varphi_0 \leq 360^\circ$  trajectories show a prevalence of outward radial pull ( $E_{\parallel} < 0$ ); in addition the motion in latitude is toward the equator for  $\varphi_0 \lesssim 270^\circ$  and toward the pole for  $\varphi_0 \gtrsim 270^\circ$ ; eventually around  $360^\circ$  the azimuthal pull prevails again.

(4) These general features are found for other initial latitudes; but the size of FS's becomes larger when moving towards the equator (see also Table I). All together these

TABLE I

Widths of forbidden sectors for electrons. Values apply approximately also to protons, but for these  $\Delta\varphi_0 \rightarrow 0$  below  $\vartheta_0 = \pi/12$  due to the negligible effect of radiation reaction

$\vartheta_0$	$\Delta\varphi_0$
$< \pi/12$	$\sim 2\pi$
$\pi/12$	$\sim \pi$
$\pi/6$	$\sim 2\pi/3$
$\pi/4$	$\sim \pi/2$
$\pi/3$	$\sim 8\pi/9$
$\pi/2$	$\sim \pi$

FS's form a 'slice' from where electrons (or protons, symmetrically) cannot leave the corotating magnetosphere. On the other hand, since trajectories from different longitudes are so dispersed, a few times  $R_c$  away the particle distribution is almost isotropic and a radially expanding uniform wind moves outward from the star.

(5) Injection at the equatorial plane ( $\vartheta_0 = \pi/2$ ), where  $\mathbf{E} \cdot \mathbf{B} = 0$  and  $E/B \lesssim 0.45$ , gives a rather peculiar situation; in fact electrons never become highly relativistic ( $v \simeq cE/B$ ). In addition, since  $B_\vartheta = 0$ ,  $B_r > B_\varphi$ ,  $E_\varphi = E_r = 0$ , electrons spiral along the equator and all move towards regions where  $B_\varphi$  is larger, slowly accelerating outward (this peculiar case was discussed as the so-called skew-wave case in Ferrari and Trussoni, 1971).

(6) Moving toward the rotation north pole, i.e. for colatitudes decreasing to zero, the FS's widen (Table I), so that no electron is allowed to escape for  $\vartheta_0 \lesssim \pi/12$ . Actually this last effect is due to radiation reaction forces which push back electrons streaming



out along the spin axis. For this reason non-total blackout exists for protons whose trajectories are not sensibly modified by radiative braking.

(7) The above results have also been tested against our choice of the light cylinder. Quite naturally an increase of the radial distance of injection narrows the width of the FS slice; in particular the selection effect completely disappears for injection distances a few times  $R_c$ . On the other hand, since particles are flowing from inside the light cylinder, the existence of the ‘slice’ actually means a spatial limitation of particle injection into the wave zone (obviously the ‘slice’ gets wider going deeper into the magnetosphere).

(8) Coming finally to the efficiency of acceleration, we first remark that, rather surprisingly, neither field structure at injection (values of  $E/B$  and  $E_{\parallel}$ ) nor subsequent behaviour of the trajectories do really influence asymptotic energies. In fact, as already discussed (Ferrari and Trussoni, 1974) Lorentz factors for electrons and protons can be shown to be related to the field by the simple relation:

$$\gamma_{as, i} = R_i^{-1} f_i \quad (i = \text{electrons or protons}), \quad (7)$$

where  $f_i$  is the field strength parameter at injection as given by Equation (3) and  $R_i$  is a reduction factor ( $2 \lesssim R_i \lesssim 10$ ) different for protons and electrons, increasing with strong radiation braking (i.e.  $f$  dependent for large  $f$ ) and only slightly dependent on field structure. Thus for chosen parameters Equation (7) gives a range  $5 \times 10^7 \lesssim \gamma_{as, el} \lesssim 9 \times 10^7$  for electrons and  $3 \times 10^4 \lesssim \gamma_{as, pr} \lesssim 2 \times 10^5$  for protons. These values are sensibly larger than for a plane wave configuration, the increment being due to near fields at the light cylinder, namely to  $E_{\parallel} \neq 0$  at injection. Actually the acceleration by a purely electric time-varying field would give  $\gamma_{as, i} = (1 + f_i^2)^{1/2}$ . This agrees with the obvious point that each trajectory meets a phase with  $E \gg B$  due to the fast rotation of the star.

Not even strongly different dynamical conditions do really modify trajectories and asymptotic energies; for instance notice that, if we inject particles with  $\gamma_0 \gtrsim \gamma_{as}$  they are initially slowed down by the rotator’s fields and then follow again the same pattern as for injection at rest. This effect is connected to  $f \gg 1$ , so that field strength completely overcomes any particle inertial motion (the case with  $\gamma_0 \gg \gamma_{as}$  is outside the classical limit).

### 3.2. OBLIQUE MAGNETIC ROTATORS

Remarkable differences from the above picture are found when considering oblique rotators, i.e. magnetic structures with axis inclined with respect to the spin axis by an angle  $\chi \neq 0$  or  $\pi/2$ .

In this case, as apparent from Equations (6), a stationary magnetic field (with  $B_{\phi} = 0$ ) is associated with the time-dependent induced electromagnetic fields and particle trajectories are peculiarly modified, in the sense that a sort of beaming of particle wind and radiation can be produced.

For this, note that the non-stationary part of the fields contains a well defined

$\varphi$ -dependence; then for any given colatitude  $\vartheta$  two distinct regions can be found: in one region (around the north magnetic pole direction) stationary and non-stationary magnetic fields add algebraically and  $|E/B| < 1$ ; in the other region they have opposite sign so that  $|E/B| > 1$  (electric fields do not change sensibly). This is expected to be an important feature, since the ratio  $E/B$  determines the particle motion to be relativistic or not because  $E_{\parallel}$  reaches full strength when  $E/B > 1$ . In Figure 4 projections of trajectories (the limits of the light cylinder were chosen as for  $\chi = \pi/2$ ) are given on a plane perpendicular to the spin axis for  $\chi = \pi/4$  and colatitude  $\vartheta_0 = \pi/4$ . A simple comparison with Figure 3 shows that the uniform distribution in azimuth is lost: a definite concentration exists around  $\varphi \approx 240^\circ$ , both for particles injected in the range  $220^\circ \lesssim \varphi_0 \lesssim 360^\circ$  (where  $E/B > 1$ ) and  $0^\circ \lesssim \varphi_0 \lesssim 60^\circ$  (where  $E/B < 1$ , but  $E_{\parallel}$  is still rather strong): in this last interval trajectories cross the light cylinder and fly above the neutron star. The width of the particle beam is  $\Delta\varphi \approx 40^\circ$  in azimuth (for protons it is rather larger) but covers all angles in latitude; therefore, it can be considered a 'knife-

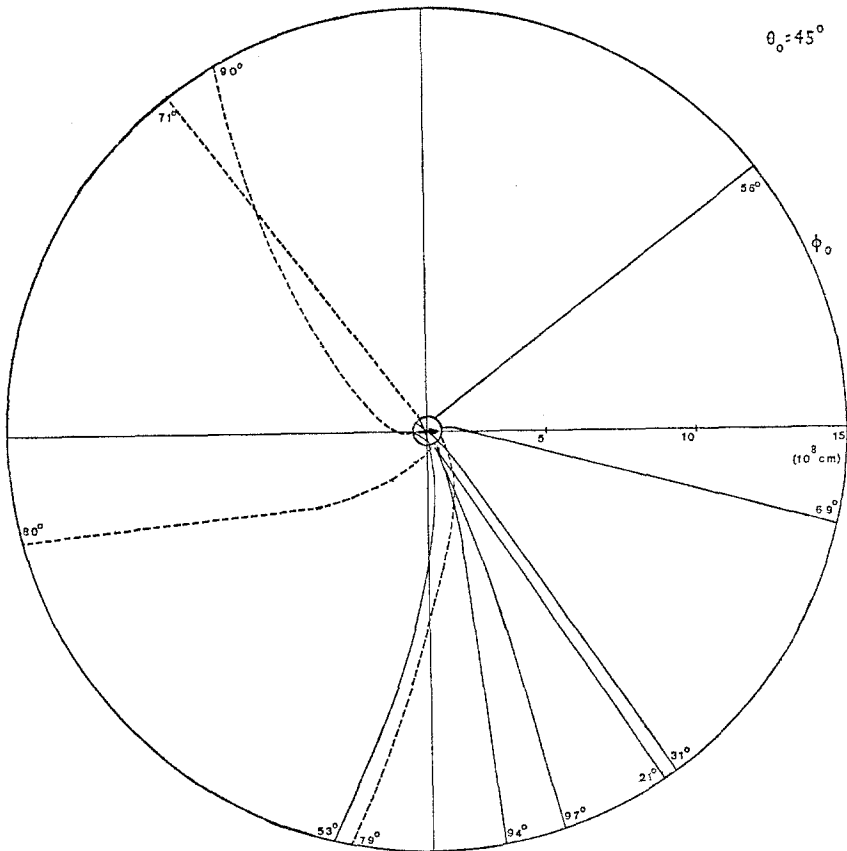


Fig. 4. Projection of asymptotic trajectories onto the equatorial plane for oblique rotators with  $\chi = \pi/4$  and  $\vartheta_0 = \pi/4$ . Power emitted by particles out of the 'beam' is negligible.

edged' beam. For injection at  $60^\circ \lesssim \varphi_0 \lesssim 180^\circ$  trajectories are rather uniform and the motion mildly relativistic ( $E_{\parallel} \ll E$ ); but we shall derive later that they contribute very poorly to radiation emission and their presence is therefore negligible. Finally, for  $180^\circ \lesssim \varphi_0 \lesssim 220^\circ$  a FS shows up again, slightly displaced from magnetic axis. The same general characteristics are found for latitudes closer to the equator (apart from the equator itself where the motion is now relativistic but all trajectories are almost radial). Conversely, for  $\vartheta_0$  decreasing towards the spin axis, FS's widen quite rapidly and for  $\vartheta_0 \lesssim 30^\circ$  no electrons escape from the light cylinder. A similar picture holds for protons with a less pronounced concentration of trajectories. Asymptotic energies do not change with respect to the case of perpendicular rotators for fixed field amplitude, as consistent with previous considerations.

Finally it is important to stress that the possibility of deriving a particle beam from inclined rotators is not related to details of their magnetic structure (apart from the assumption of axial symmetry), but is quite general as due to the interaction of stationary and induced fields.

#### 4. Synchro-Compton Emission and Spectrum

The radiated power of relativistic charges accelerated by a strong electromagnetic field is given by

$$P = r_e \tau_0 \gamma^2 [(c\mathbf{E} + \mathbf{v} \times \mathbf{B})^2 - (\mathbf{v} \cdot \mathbf{E})^2].^* \quad (8)$$

Rather difficult is a complete spectral analysis of this radiation via Fourier transforms, since details of trajectories should be used. On the other hand this spectrum is strongly peaked, and we shall simply study its maximum at each point along the trajectory.

Then this critical frequency can be written as

$$\omega_c = \frac{eF_{\perp}}{mc} \gamma^2 \quad (\gg \omega), \quad (9)$$

where

$$eF_{\perp} = e \left| \frac{\mathbf{v}}{v} \times \left( \mathbf{E} + \frac{\mathbf{v}}{c} \times \mathbf{B} \right) \right| \quad (10)$$

is the perpendicular force acting on the moving charge. An appreciable emission of radiation along with particle acceleration has to be expected, since radiation reaction forces have been shown to affect trajectories significantly (see also Ferrari and Trussoni, 1974).

In Figures 5 and 6 typical results are plotted for protons and electrons caught by the

\* Discussion has arisen about a relativistic 'piling-up' of radiation in the observer frame, so that the received energy should be  $\approx \gamma^2 \times P$ .

Nevertheless this appears to be true only for continuous sources, while for single electrons no correction would be needed (see also Kegel, 1971).

wave at  $\vartheta_0=45^\circ$ ,  $\varphi_0=90^\circ$  in the case of perpendicular rotators. In young pulsars one single electron radiates up to  $\approx 200$  erg (mainly in the early phase,  $\Delta t \approx 10^{-1}$  s) at a frequency typically of the order of  $\approx 10^{23+24}$  c s $^{-1}$  and radiation is strictly collimated along its trajectory; for old pulsars with the same surface field (magnetic decay time  $\gg$  slowing-down time scale), these values are scaled down as  $P \propto \omega^{10}$  and  $\omega_c \propto \omega^7$  approximately (structure of fields and radiation braking do actually slightly affect these laws).

Initial dynamical conditions can largely increase the above values; as shown again in Figures 5 and 6, for  $\gamma_0 \approx \gamma_{as}$  one would obtain  $E \approx 260$  erg and  $\omega_c \approx 10^{26}$  c s $^{-1}$  (in the initial portion of trajectories), i.e. in the initial part of the motion particles can

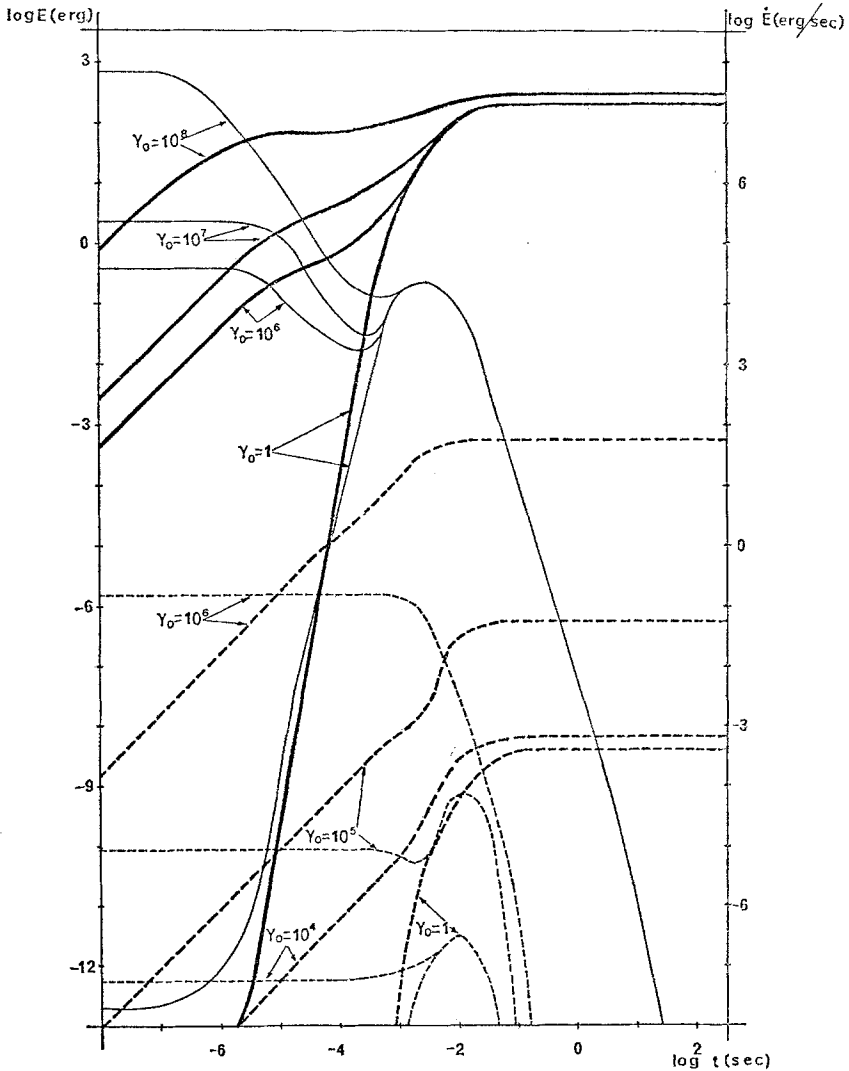


Fig. 5. Emitted power  $\dot{E}$  (light lines) and total emitted energy  $E$  (heavy lines) for electrons (full lines) and protons (dotted lines) injected at different initial energies for the case  $\chi=\pi/2$  and  $\vartheta_0=\pi/4$ .

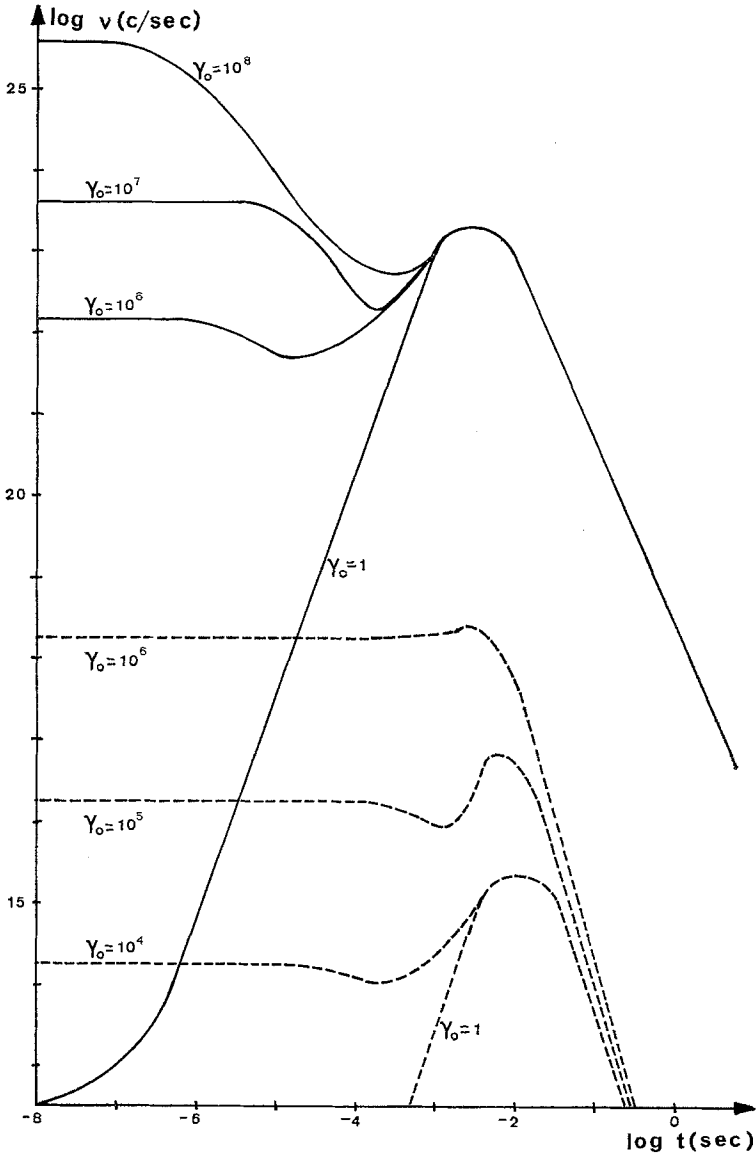


Fig. 6. Peak frequency of the spectrum for electrons (full lines) and protons (dotted lines) along the trajectories for  $\chi = \pi/2$  and  $\vartheta_0 = \pi/4$ ; various initial energies are represented.

radiate about 20% of their total output in very high energy  $\gamma$ -rays. It is also clear that protons themselves are powerful emitters and for relativistic speed at injection they radiate soft X-rays.

In the case of perpendicular rotators these considerations are valid for all injection points, apart from the equatorial plane where the motion is bound to be mildly relativistic. The overall picture is partly different for oblique rotators; the above values are

reached only by those particles which are in the beam: all other particles give powers lower by  $\frac{1}{2}\theta \div \frac{1}{3}\theta$  (in the soft X-ray region). Therefore an oblique rotator model can actually provide anisotropic emission of high-frequency radiation as requested in fastest pulsars; this holds for all magnetic rotators with axial symmetry and details of their structure determine the pattern of emitted pulses.

## 5. Conclusions

In this last section we shall discuss an application of our results to the interpretation of pulsed high-frequency radiation from NP 0532. We divide our analysis in three parts concerning: (i) formation of radiation pulses; (ii) spectrum of radiation; (iii) limits of validity of electrodynamic models. In a separate paper we have studied the implications of the acceleration process with high-energy cosmic-ray production (Ferrari and Trussoni, 1974).

(i) *Radiation pulses.* We start from the idea that in the magnetosphere of rotating collapsed stars with axially symmetric surface field, flux lines exist which do not close on the star and bring electric charges at the upper boundary of the corotating region. In particular we can assume that an isotropic supply of electrons (and ions) comes to the light cylinder, from where they undergo acceleration and radiate through the synchro-Compton mechanism. When the magnetic structure is oblique to the rotation axis, trajectories of accelerated electrons are collimated in narrow beams and the same is true for radiation emitted close to  $R_c$  which, due to star rotation, becomes pulsed for any observer lying along their line of sight. Incidentally we recall that these beams are limited in longitude, but are rather wide in latitude, cutting a sort of 'slice' in the light cylinder; therefore the probability of observing such a pulsar is in principle very high. Quite naturally details of pulse shape, interpulses, drifting subpulses would directly depend on the magnetic structure of the star and its magnetosphere. This last, for instance, could directly affect particle supplies into the radiation zone, since forbidden sectors do actually widen below  $R_c$ .

A question should now be asked: how large must the electron supply at the light cylinder be to level off the received power, as estimated from observations? Referring to NP 0532 we know (see, for instance, Kurfess, 1971) that the emitted power in high-frequency pulses (hard X-soft  $\gamma$  rays) should be  $\approx 5 \times 10^{36}$  erg s $^{-1}$  (assuming isotropic emission); in addition particle flux across the light cylinder is bound to be  $10^{33} \lesssim \dot{\varphi} \lesssim 10^{41}$  part s $^{-1}$ : the upper limit is established by the slowing-down rate of the period and the lower by the minimum charge density requested to maintain a quasi-stationary magnetosphere around the star (Ruderman, 1972).

Then our previous results on radiation by electrons ( $\dot{E} > 10^3$  erg s $^{-1}$ ) show that particle fluxes needed to justify the observed luminosity via synchro-Compton at  $R_c$  are rather low, roughly  $\sim 10^{34 \div 35}$  p s $^{-1}$  even considering reduction factors related to the narrow beam structure, so that we expect to find a not too dense magnetosphere. Another aspect of pulsar energetics should also be noticed: pulsed radiation is  $\approx \frac{1}{2}\theta$

only of total pulsar energy losses as derived from slowing-down rate and dynamics of the nebula. This would be consistent with the assumption that the low-frequency wave is not strongly refracted by the synchro-Compton interaction in the zone of the light cylinder, so that a single particle treatment is justified.

(ii) *Spectrum of pulsed radiation.* Data from NP 0532 suggest that pulses have a relatively large peak in the range  $\nu \approx 10^{19+23} \text{ c s}^{-1}$  with a tail up to  $\nu \sim 10^{26} \text{ c s}^{-1}$  (see Kurfess, 1971; McBreen *et al.*, 1973; Helmken *et al.*, 1973). Our results would support a somewhat narrower frequency peak, i.e.  $\nu \approx 10^{23+24} \text{ c s}^{-1}$ , on the basis of the standard set of pulsar parameters. This apparent discrepancy could be actually rounded off in different ways. First of all by further reducing  $B_s$  at the surface of the collapsed star ( $\nu \propto B_s^3$ ) with suitable conditions on particle initial velocities (see below) or alternatively assuming a somewhat wider light cylinder ( $r \approx 2 R_c$ ), in connection with the influence of plasma collective effects delaying acceleration processes at the limits of the corotating magnetosphere.

Concerning the high-frequency tail of the spectrum, its intensity can be easily accounted for if just a small fraction of the electrons ( $\approx 10^{-3}$  of total particle flux) is caught by the wave slightly closer to the star, or with  $\gamma_0 \lesssim \gamma_{as}$ . Conversely synchro-Compton emission does not seem suitable for highly coherent pulses emitted in radio and optical bands; neither electrons nor protons (see Figures 5 and 6) would give an appreciable power. Emission in these frequency ranges is likely to be connected with plasma resonant processes close to the star (Coppi and Ferrari, 1970) or MHD instabilities at the boundaries of the corotating magnetosphere.

Finally referring to Vela pulsar, we see that the strong dependence of power and spectrum on rotation frequency suggests that the high-frequency phase of pulsars is very short; then in this case ( $\omega \approx 12 \text{ c s}^{-1}$ ) we can still fit observations of pulsed hard X-rays ( $\nu \approx 10^{19} \text{ c s}^{-1}$ ; see Harnden *et al.*, 1972; or Cruise and Newton, 1973). For slower pulsars radiation pulses in these bands would not be detectable.

(iii) *Reliability of electrodynamic models.* Magnetic rotator models for pulsars meet difficulties in interpreting correctly the slowing-down index,  $n = \ddot{\omega}\omega/\dot{\omega}^2$  which for NP 0532 has been measured to be  $\approx 2.5$  (Groth, 1974). In fact electromagnetic losses would give  $n=3$  for vacuum dipole rotators and larger values for higher multipoles. On the other hand it is rather evident, as suggested by Ruderman (1972), that the outflow of plasma from the magnetosphere could actually reduce the theoretical index by modifying the law of energy and angular momentum losses. Then a clear solution of this problem would require a self-consistent theory of electrodynamics around collapsed stars, where electromagnetic fields are very far from simple approximations of spherical or plane wave. Incidentally we recall that this correct solution would also be essential to define the near fields which actually drive the beaming effect itself. In this respect a qualitative simple consideration about the possible influence of a non-negligible plasma distribution should be that the inertia of particles (ions) trapped by magnetic lines could develop a toroidal component in addition to the one induced by rotation; this effect should be relevant for dense magnetospheres only. Eventually in

this situation corotation could be lost at  $r \approx V_A/\omega \lesssim R_c$  and acceleration would start with much stronger near fields.

In conclusion we summarize our results in two main points. (1) We do expect that, independently of the magnetic structure of the rotator and its magnetosphere, regions where  $\mathbf{E} \cdot \mathbf{B} = 0$  and  $|\mathbf{E}| \neq |\mathbf{B}|$  are always present in analogy with the vacuum solution. This means that acceleration process and synchro-Compton emission at high frequency do always take place. (2) Details of magnetic structure determine the beaming effect for which axial symmetry in oblique rotators is required; high-frequency sources are therefore pulsed only when those geometrical relations are fulfilled: quite a reasonable possibility, allowing a general agreement with observations.

### Acknowledgements

The authors would like to thank R. M. Kulsrud and G. Silvestro for comments and discussions.

This work was partially supported by the Consiglio Nazionale delle Ricerche under Contract 73.00251.02.

### References

- Blandford, R. D. and Rees, M. J.: 1972, *Astrophys. Letters* **10**, 77.  
 Coppi, B. and Ferrari, A.: 1970, *Astrophys. J. Letters* **161**, L65.  
 Cruise, A. M. and Newton, A. C.: 1973, *Nature Phys. Sci.* **244**, 121.  
 Deutsch, A.: 1955, *Ann. Astrophys.* **18**, 1.  
 Ferrari, A. and Trussoni, E.: 1971, *Lett. Nuovo Cimento* **1**, 137.  
 Ferrari, A. and Trussoni, E.: 1973, *Astrophys. Space Sci.* **24**, 3.  
 Ferrari, A. and Trussoni, E.: 1974, *Astron. Astrophys.*, in press.  
 Grewing, M. and Heintzmann, H.: 1971, *Astrophys. Letters* **8**, 167.  
 Groth, E.: 1974, *Astrophys. J.*, in press.  
 Gunn, J. E. and Ostriker, J. P.: 1971, *Astrophys. J.* **165**, 523.  
 Harnden, F. R., Johnson, W. N., and Hajmes, R. C.: 1972, *Astrophys. J. Letters* **172**, L91.  
 Helmken, H. F., Fazio, G. G., O'Mongain, E., and Weekes, T. C.: 1973, *Astrophys. J.* **184**, 245.  
 Kegel, W. H.: 1971, *Astron. Astrophys.* **15**, 306.  
 Kurfess, J. D.: 1971, *Astrophys. J. Letters* **168**, L39.  
 McBreen, B., Ball, S. E., Campbell, M., Greisen, K., and Koch, D.: 1973, *Astrophys. J.* **184**, 571.  
 Ostriker, J. P. and Gunn, J. E.: 1969, *Astrophys. J.* **157**, 1395.  
 Rees, M. J.: 1971a, *Nature* **229**, 312.  
 Rees, M. J.: 1971b, *Nature Phys. Sci.* **230**, 55.  
 Ruderman, M.: 1972, *Ann. Rev. Astron. Astrophys.* **10**, 427.